

Streamflow drought time series forecasting

Reza Modarres

Published online: 1 July 2006
© Springer-Verlag 2006

Abstract Drought is considered to be an extreme climatic event causing significant damage both in the natural environment and in human lives. Due to the important role of drought forecasting in water resources planning and management and the stochastic behavior of drought, a multiplicative seasonal autoregressive integrated moving average (SARIMA) model is applied to the monthly streamflow forecasting of the Zayandehrud River in western Isfahan province, Iran. After forecasting 12 leading month streamflow, four drought thresholds including streamflow mean, monthly streamflow mean, 2-, 5-, 10- and 20-year return period monthly drought and standardized streamflow index were chosen. Both observed and forecasted streamflow showed a drought period with different severity in the lead-time. This study also demonstrates the usefulness of SARIMA models in forecasting, water resources planning and management.

Keywords Hydrologic time series · SARIMA model · Drought · Forecasting · Threshold definition · Zayandehrud River

1 Introduction

1.1 Background

Drought is considered as the most complex natural phenomenon and, at the same time, the least under-

stood among natural hazards with different temporal and spatial characteristics. Drought generally involves long and sustained periods with insufficient precipitation, soil moisture or water resources for supplying the socio-economic activities in a region. Wilhite and Glantz (1985) and Wilhite et al. (1986) have shown that the lack of a precise definition of drought has been an obstacle in understanding drought. This has led to indecision and inaction on the part of managers and policy makers. Perhaps the first efforts to predict drought was carried out by Yevjevich (1967) by the means of probability distribution. The use of run theory in drought forecasting was introduced by Sen (1976, 1977). Stochastic nature of drought has also been studied by many investigators. The renewal processes was applied by Loaiciga and Leipnik (1996) to model the occurrence of drought events. Lohani and Loganathan (1997) used Palmer drought severity index (PDSI) in a non-homogenous Markov chain model to characterize the stochastic behavior of drought. Chung and Salas (2000) used low-order discrete autoregressive moving average models for estimating the occurrence probabilities of drought events. Kim and Valdes (2003) used PDSI as drought parameter to forecast drought in the Conchos River basin in Mexico using conjunction of dyadic wavelet transforms and neural network. Recently, Mishra and Desai (2005) applied seasonal autoregressive integrated moving average model to forecast standardized precipitation index (SPI).

1.2 Stochastic hydrologic modeling

During the past five decades, several studies have developed methods of analyzing stochastic characteristics of hydrologic time series (i.e., Delleur et al. 1976;

R. Modarres (✉)
Natural Resources Faculty,
Isfahan University of Technology, Isfahan, Iran
e-mail: r_m5005@yahoo.com

Salas and Obeysekera 1982; Hipel 1993; Hanson et al. 2004; Yurekli et al. 2005).

Perhaps the most widely used model is the ARIMA model (Box and Jenkins 1976). The two general forms of ARIMA models are non-seasonal ARIMA(p, d, q) and multiplicative seasonal ARIMA(p, d, q) \times (P, D, Q) in which p and q are non-seasonal autoregressive and moving average, P and Q are seasonal autoregressive and moving average parameters, respectively. The other two parameters, d and D , are required differencing used to make the series stationary.

The differencing operator that is usually used in the case of non-stationary time series is $\nabla = 1 - B$ (B is backward shift operator) and $\nabla^d = (1-B)^d$ for seasonal differencing. This form of non-seasonal ARIMA(p, d, q) is written as

$$\phi(B)Z_t = \phi(B)(1 - B)^d Z_t = \theta(B)a_t \quad (1)$$

where Z_t is the observed series, $\phi(B)$ is the polynomial of order p and $\theta(B)$ is the polynomial of order q .

For seasonal time series that contain cyclic features, seasonal differencing is often applied. In this case we have a multiplicative model given by

$$\phi_p(B)\Phi_P(B^S)\nabla^d\nabla_s^D(Z_t - \bar{Z}) = \theta_q(B)\Theta_Q(B^S)a_t \quad (2)$$

where Φ_P and Θ_Q are seasonal polynomials of order P and Q , respectively. This is the general form of the multiplicative seasonal ARIMA model of order (p, d, q) \times (P, D, Q).

1.3 Case study

The Zayandehrud River basin is located in the central part of Iran at the eastern hillslope of Zagros

Mountains and western region of Isfahan province. Plasjan basin with the area of about 1,600 km² is the main unregulated watershed of Zayandehrud basin and is directly connected to Zayandehrud reservoir, which has an important role in water supplying for Isfahan city. The rainfall regime is typically Mediterranean with about 1,400 mm annual rainfall. Generally, rainfall is rare from June to August when the temperature can reach to 38°C. In the last years of 20th century (1998–2001), drought occurred in Iran which resulted in a high socio-economic damage. The water storage of Zayandehrud dam decreased to the lowest level during 25 years. The main objective of the present study is to develop a valid stochastic model to forecast streamflow drought in the major river flow of Zayandehrud River which mainly provides the water storage of Zayandehrud dam. The physical area considered in this study is shown in Fig. 1.

2 Methodology

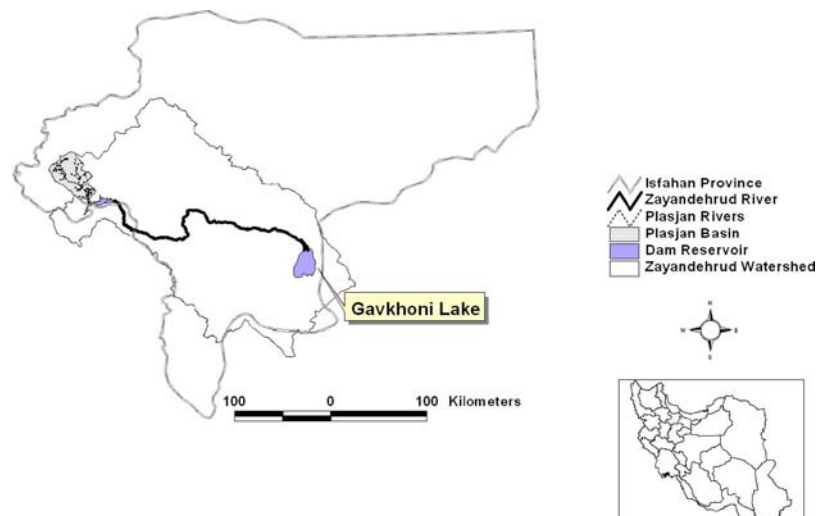
2.1 Time series modeling

The Box and Jenkins (1976) modeling approach involves the following three steps:

2.1.1 Model identification

In this step, the model that seems to represent the behavior of the series is searched, by the means of autocorrelation function (ACF) and partial autocorrelation function (PACF), for further investigation and parameter estimation. The behavior of ACF and PACF, is to see whether the series is stationary or not,

Fig. 1 Location of Plasjan basin in Zayandehrud watershed



seasonal or non-seasonal. Differencing is done to make non-stationary time series to stationary time series.

2.1.2 Parameter estimation

After identifying models, we need to obtain efficient estimates of the parameters. These parameters should satisfy two conditions namely stationary and invertibility for autoregressive and moving average models, respectively (Box and Jenkins 1976; Salas et al. 1980; Bowerman and O’Connell 1993).

The parameters should also be tested whether they are statistically significant or not. Associated with parameters value are standard errors of estimate and related *t*-values.

If θ is the point estimate of the population parameter, θ , and S_θ denotes the standard error of θ , the *t*-value is calculated by

$$t = \frac{\theta}{S_\theta} \tag{3}$$

If the hypothesis $H_0\theta = 0$ is rejected in favor of $H_0\theta \neq 0$ by setting the probability of type I error equal to $\alpha = 0.05$ or $\alpha = 0.05$, the parameter is significant and is kept in the model.

2.1.3 Goodness-of-fit test

Goodness-of-fit tests verify the validity of the model by some tools. The residuals of the model are usually considered to be time-independent and normally distributed over time. The most common tests applied to test time-independence and normality are the Port Manteau lack of test, the non-parametric Kolmogorov–Smirnov test.

The Portmanteau lack of test (Salas et al. 1980) compute a statistic, Q^* , which is approximately distributed as $\chi^2(l-p-q)$ and is given by

$$Q^* = n'(n' + 2) \sum_{e=1}^k (n' - l)^{-1} r_e^2(\hat{a}) \tag{4}$$

where $n' = n - d$, Q^* has $k - n_p$ degrees of freedom where k is the lag number, n is the number of observation and d is required differencing. If the probability of Q is less than $\alpha = 0.01$, there is strong evidence that the model is inadequate and if this probability is greater than $\alpha = 0.05$, it is reasonable to conclude that the model is adequate.

The residuals of the model must also be normal. The well-known non-parametric test is Kolmogorov–Smirnov test (Hollander and Wolfe 1999) given by

$$D = \text{Max}|F(x) - F_0(x)| \tag{5}$$

where D is Kolmogorov–Smirnov’s statistic, $F(x)$ the cumulative distribution functions (cdf) of observations, $F_0(x)$ the cdf of assumed distribution which is normal distribution herein and N the number of data. If the value of statistic is smaller than the critical value, the null hypothesis $H_0:F(x) = F_0(x)$ is accepted in favor of $H_0:F(x) \neq F_0(x)$ and this means that residuals of the model are normally distributed in time and also adequate for modeling. Another graphical test for normality is cumulative periodogram (Hipel and McLeod 1994).

Another important characteristic of residual is homoscedasticity which means no change in variance of the residual. The following test described by Breusch and Pagan (1979) is very useful to determine heteroscedasticity of residuals. For the test, the residuals from the model fit to the data are divided into two groups with the sample sizes of n_s and n_p . Then, residual sum of squares of the first (ESSF) and second (ESSS) groups are obtained. Breusch–Pagan test statistic (F_{cal}) is obtained from the following equation (Yurekli et al. 2005).

$$F_{\text{cal}} = \frac{\text{ESS}_s / (n_s - k_p)}{\text{ESS}_f / (n_f - k_p)} \approx F_{\text{table}}[(n_s - k_p), (n_f - k_p)] \tag{6}$$

where k_p is the degree of freedom. If F_{cal} is smaller than F -table critical value, the residuals are assumed to be homoscedastic.

2.1.4 Parameter uncertainty analysis

This section describes uncertainty assessment used in this study in analyzing uncertainties of model parameter, θ_s . The uncertainty is assessed with the comparison of means of the parameters of synthetic monthly streamflow series with the parameters of the fitted model. In this study, the comparison consists of three steps. Firstly, 100 random samples, each of size $n = 1,200$ monthly streamflow, were simulated. In the second step, the model estimated through Sects. 2.1.1–2.1.3, is fitted to the synthetic series and their parameters are estimated. In the third step, a bootstrap simulation is used to estimate the uncertainty (bias and variance) associated with the sample estimate. In the standard version of bootstrap (Efron and Tibshirani 1993), a random sample of size n is drawn with replacement from the ordered sample $\{X_{1:n}, X_{2:n}, \dots, X_{n:n}\}$ as

$$X_j^* = F_E^{-1}(p) = X_{(np)+1} \quad \text{for } j = 1, n \quad (7)$$

where $F_E^{-1}(p)$ denotes the empirical (sample) quantile function, p is a uniform rv(0–1) and (np) denotes the integer floor function. Using a k th bootstrap sample, denoted by

$$X^*(K) = \{X_1^*, X_2^*, \dots, X_n^*\} = 1, 2, \dots, b \quad (8)$$

a new bootstrap estimate θ_k^* of θ_s can be obtained. Here, b denotes the number of bootstrap simulations. The set of estimates, $\theta^* = \{\theta_1^*, \theta_2^*, \dots, \theta_b^*\}$ constitutes the sampling distribution of θ_s . The bootstrap estimate of the true bias ($E[\theta_s] - \theta$) is given as

$$\text{Bias} = (\theta_m^* - \theta_s) \quad (9)$$

Where θ_m^* is the average of all bootstrap estimates θ^* . The variance of θ^* is estimated as

$$\text{Variance} = (\text{standard error})^2 = \frac{1}{b-1} \sum_{k=1}^b (\theta_k^* - \theta_m^*)^2 \quad (10)$$

2.1.5 Model calibration

In order to evaluate the accuracy of the streamflow forecasts obtained by applying the fitted model, the following tests are used in this study.

- computing correlation coefficients between observed and forecasted series
- computing the corresponding coefficient of efficiency (Brath and Rosso 1993),

$$E = 1 - \frac{\sum (Q_t - \hat{Q}_t)^2}{\sum (Q_t - \bar{Q})^2} \quad (11)$$

where \hat{Q}_t is the discharge at time t forecasted with a given lead-time, Q_t is the corresponding observed streamflow and \bar{Q} is the mean of the whole series of the observed streamflow.

- The root mean squared errors (RMSEs) for forecasted streamflow,

$$\text{RMSE} = \left(\frac{\sum_{i=1}^n (F_i - O_i)^2}{n} \right)^{1/2} \quad (12)$$

where F_i and O_i are forecasted and observed streamflow.

- Non-parametric test for the difference of observed and forecasted streamflow means by the use of

Wilcoxon rank sum method (Conover 1980; Khan et al. 2006). It is the best robust non-parametric methods for constructing a hypothesis test P -value for difference of two population means ($\mu_1 - \mu_2$). At any significant level less than P -value, the null hypothesis, equality of the population and model parameter, is rejected.

- Non-parametric test for the equality of observed and forecasted streamflow variances by the use of Levene's test (Levene 1960).
- Kolmogorov–Smirnov non-parametric goodness-of-fit test to compare cdf of observed and forecasted series (Sect. 2.1.3).

2.2 Drought definitions and thresholds

Drought is generally considered as periods with insignificant precipitation, soil moisture and water resources for sustaining and supplying the socio-economic activities of a region. Thus, it is difficult to give a universal definition of drought (Loukas and Vasilades 2004). The most well-known classification of droughts is the classification proposed by Dracup et al. (1980). The American Meteorological Society (2004) adopted this drought classification system. These classifications which are based on the nature of the water deficit are defined: (a) the meteorological drought, (b) the hydrological drought, (c) the agricultural drought, (d) the socio-economic drought. It is necessary, for the analysis of any kind of above droughts, to select an appropriate indicators for defining droughts. Almost all drought indices are based on the basic method of truncation used to derive drought events from continues or discrete records of streamflow, precipitation, temperature, ground water drawdown and lake elevation (Chang and Kleopa 1991). A drought is defined as an uninterrupted sequence of streamflow below an arbitrary level (Yevjevich 1967). The streamflow denoted by x_i where i indicates the time and the arbitrary level, called the truncation level and denoted by x_0 , is assumed to be constant. Examples of applied truncation level are the mean (Bonacci 1993), the median (Griffiths 1990), mean and 75% of the mean (Clausen and Pearson 1995) and lower percentage exceedances, e.g., 90 or 95% flows found from flow duration curves (Zelenhasic and Salvai 1987; Chang and Stenson 1990). Thus the mean value of streamflow time series is selected as the first truncation level. In the present study, as the monthly streamflow time series is applied for drought forecasting, the monthly mean values are also applied as the truncation level for each month. Besides

the two above truncation levels, we apply two other drought indices called standardized streamflow index (SSFI) and a probabilistic index which is based on hydrologic drought return periods.

Standardized streamflow index is statistically similar to the other most commonly used SPI introduced by McKee et al. (1993) for meteorological drought analysis. The SSFI for a given period is defined as the difference of streamflow from mean divided to standard deviation (McKee et al. 1993) as follows

$$SSFI = \frac{F_i - \bar{F}}{\sigma} \tag{13}$$

in which, F_i is flow rate in time interval i , \bar{F} is the mean of the series and σ is the standard deviation of the series. For monthly series, the SSFI is written as follows:

$$SSFI_{\tau} = \frac{F_{v\tau} - \bar{F}_{\tau}}{\sigma_{\tau}} \tag{14}$$

in which

$$\bar{F}_{\tau} = \frac{1}{n} \sum_{v=1}^N F_{v,\tau}, \quad \tau = 1, \dots, \omega \tag{15}$$

$$\sigma_{\tau} = \sqrt{\frac{1}{n-1} \sum_{v=1}^n (F_{v,\tau} - \bar{F}_{\tau})^2} \tag{16}$$

where v denotes the year and τ denotes the interval within year, \bar{F}_{τ} and σ_{τ} are mean and standard deviation of month τ and $\omega = 12$.

The fourth drought threshold used in this study is the probability (or equivalent return period) with which a certain drought will be equaled or not exceeded in the base period of record. Rainfall, streamflow, flood and low flow frequency analysis is a major task for hydrologic designers and planners. In this study, many distributions are fitted to monthly streamflow of Zayandehrud River to estimate hydrologic drought in different return periods ($T_{\tau} = 1/1$ -non-exceedance probability).

3 Results and discussions

3.1 Stochastic modeling

A stochastic linear ARIMA model is fitted to Plasjan River, the main branch of Zayandehrud River. Monthly streamflow time series of this river is used in the period of January, 1970 to December, 1999

($i = 1, \dots, 360$; Fig. 2). Table 1 shows basic statistical features of the streamflow of Plasjan River.

In the first step of model identification, the ACF and PACF of the actual data indicate the need of differencing. However, Fig. 3 shows the $Q-Q$ plot of the main series does not show normality. Thus, the logarithmic transformation was applied. The transformed $Q-Q$ plot shows that the new series is normal (Fig. 3). Two other non-parametric Kolmogorov–Smirnov and chi-square tests of normality were also done for the logarithmic series. The null hypothesis of normality is accepted at 5% level as the K–S and chi-square statistics of the logarithmic series, $D = 0.093$ and $\chi^2 = 67.15$, are smaller than critical values, $D = 0.12$ and $\chi^2 = 70.12$, respectively.

The ACF and PACF of the seasonal and non-seasonal differenced logarithmic series ($D = 1$ and $d = 1$) are shown in Figs. 4 and 5. Two models were initially selected, ARIMA(1, 1, 1) \times (0, 1, 1) and ARIMA(1, 1, 1) \times (1, 1, 1).

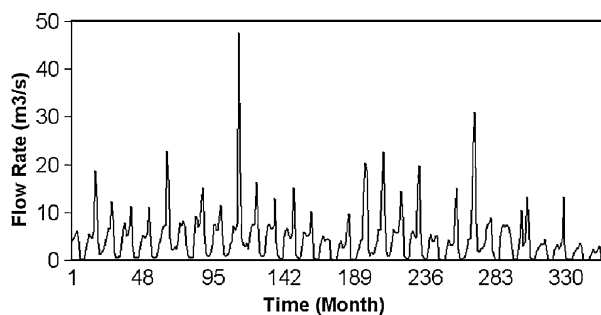


Fig. 2 Time series of monthly streamflow of Plasjan River (1970–1999)

Table 1 Summary of monthly and annual statistical properties of Zayandehrud streamflow (1970–1999)

Months	Mean (m ³ /s)	Standard deviation (m ³ /s)	Coefficient of variation (%)	Skewness	Kurtosis
January	5.12	1.60	31.16	-0.21	-1.01
February	5.20	1.56	29.99	-0.04	-1.16
March	7.67	3.49	45.47	0.91	-0.02
April	13.56	8.85	65.27	2.09	6.74
May	7.66	7.07	92.32	1.59	2.95
June	1.51	1.69	112.05	2.23	5.62
July	0.67	0.72	107.29	2.21	5.29
August	0.62	0.68	109.66	1.59	2.29
September	0.85	0.90	105.89	1.46	1.76
October	2.59	1.35	52.23	0.46	-0.01
November	4.29	1.98	46.18	0.50	-0.28
December	5.39	2.02	37.57	0.34	-0.07
Annual	4.59	1.87	40.76	0.60	0.49

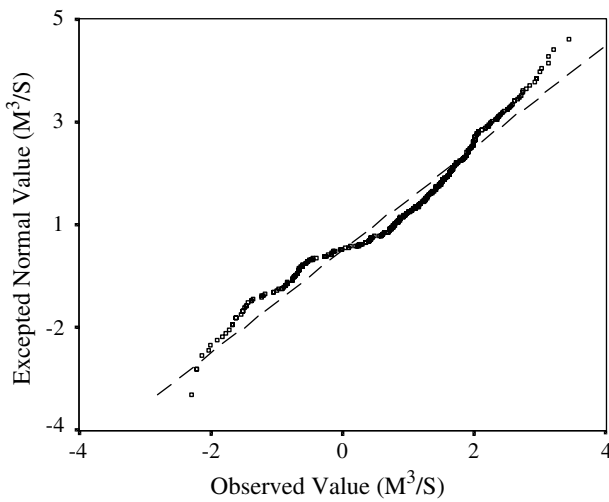


Fig. 3 QQ plot of observed logarithmic series

The ARIMA(1, 1, 1) × (0, 1, 1) model is rejected because the non-seasonal moving average parameter is not significant. The same condition is true for the seasonal autoregressive parameter of ARIMA(1, 1, 1) × (1, 1, 1) model. As non-seasonal moving average and seasonal autoregressive are not significant in previous models, we leave out these models and try ARIMA(1, 1, 0) × (0, 1, 1) as the third model which can pass this step. The statistical analysis of model parameters is presented in Table 2. The bias and standard error of the 1,000 bootstrap simulations show the validity of the model parameters. The average values of the parameters estimated from bootstrap are 0.872 and 0.761 for autoregressive and moving average parameters, respectively, which are very close to the exact values (0.87 and 0.76). In a sense, parameter estimates of the fitted model, ARIMA(1, 1, 0) × (0, 1, 1), are almost unbiased.

The results of Porte Manteau lack-of-fit test indicate that the residuals of the third model are time-independent. Figures 6 and 7, residual ACF and PACF of the models, do not show significant autocorrelation coefficient. The Kolmogorov–Smirnov and heteroscedasticity Breusch–Pagan test statistic are 0.118 and 0.93, respectively, which satisfy normality and homogeneity of the residuals. The cumulative periodogram (Fig. 8) also indicates that the residuals are time-independent. Thus, the third model is accepted for streamflow forecasting. The selected ARIMA(1, 1, 0) × (0, 1, 1) model is written

$$0.76(B)\nabla^1\nabla_{12}^{12}Z_t = -0.87(B^{12})a_t \tag{17}$$

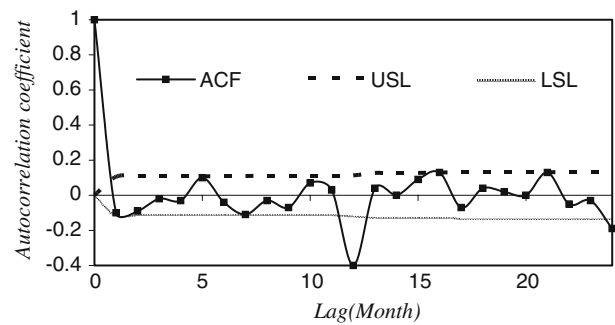


Fig. 4 ACF of logarithmic and seasonal and non-seasonal differenced series (USL upper significant level, LSL lower significant level)

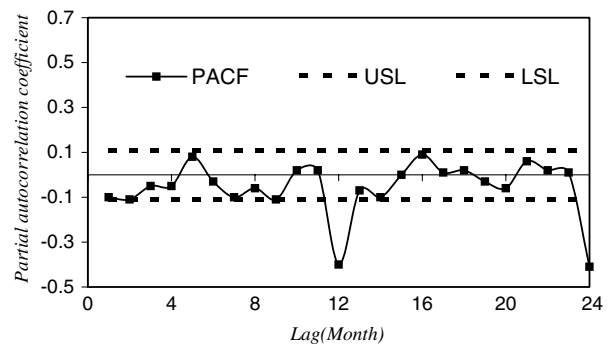


Fig. 5 PACF of logarithmic and seasonal and non-seasonal differenced (USL upper significant level, LSL lower significant level)

3.2 Model calibration

For testing the validity of the above model for forecasting, the model is used for forecasting 9-, 3- and 1-year monthly streamflow. We call these forecasting periods scenario 1, 2 and 3, respectively. Thus, in the first scenario, the model is used to forecast $9 \times 12 = 108$ monthly streamflow for the period of January 1990 to December 1999. In the second scenario, the model is used for forecasting monthly streamflow in the period of January 1997 to December 1999. In the third scenario, the model is used for forecasting monthly streamflow for the period of January 1999 to December 1999. The methods described in Sect. 2.1.5 are then used to calibrate the model for forecasting. The results of these methods are presented in Table 3. As this table shows, the difference between observed and forecasted streamflow is significant for the first scenario. Although the correlation coefficient is significant at 95% level but it does not show a satisfactory forecasting in comparison with two other

Table 2 Result of parameter estimation and bootstrap analysis for the third model, ARIMA(1, 1, 0)(0, 1, 1)

Parameters	Values	Standard error (SE)	t-Ratio	P < 0.01	Bootstrap			
					Variance		Mean	
					SE	Bias	SE	Bias
ϕ_1	0.87	0.04	21.03	0.0001	0.00032	-0.000032	0.0042	0.000058
Θ_1	0.76	0.05	22.4	0.0001	0.00093	-0.000074	0.0081	0.000058

scenarios. The coefficient of efficiency is also very low which shows an unsatisfactory streamflow forecasting for 9 years. The RMSE of the forecasting streamflow for the first scenario is relatively higher than the second

scenario and the RMSE of the second scenario is also relative higher than the third scenario. This indicates that the model is relatively suitable for streamflow forecasting for 12 months ahead.

The other statistics which compare the statistic properties of observed and forecasted streamflow also show the significant difference between the mean, variance and distribution of the observed and the forecasted streamflow in the first scenario. The same conditions can be seen for the second scenario in which 3-year monthly streamflow has been forecasted. However, in the third scenario in which 1-year monthly streamflow has been forecasted, the statistics show that there is not significant difference between observed and forecasted streamflow. The correlation coefficient and the coefficient of efficiency are significantly high and indicate a very satisfactory forecasting. The P-values of Wilcoxon and Levene’s tests are higher than 0.05. This demonstrates that there is not significant difference between observed and forecasted streamflow mean and variance. The Kolmogorov–Smirnov statistics also demonstrate that there is no significant difference between observed and forecasted distribution function. Thus, we can conclude that the model is valid for forecasting 1-year ahead monthly streamflow which is the aim of this study for drought forecasting.

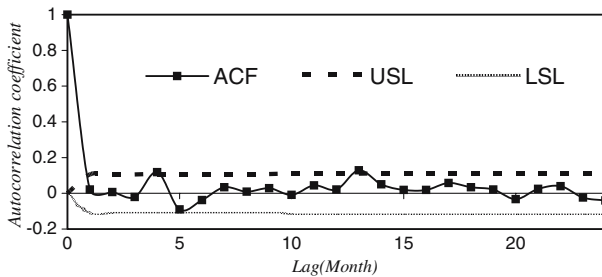


Fig. 6 Residuals’ ACF of the model estimated by ULS method (USL upper significant level, LSL lower significant level)

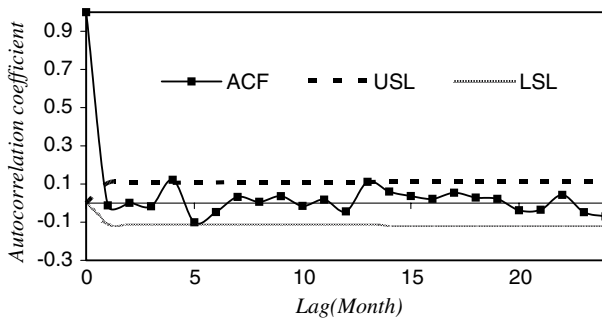


Fig. 7 Residuals’ ACF of the model estimated by ML method (USL upper significant level, LSL lower significant level)

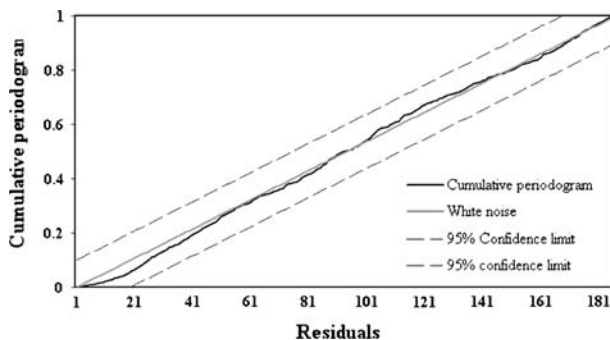


Fig. 8 Cumulative periodogram and 95% confidence limits for monthly streamflow of Zayandehrud River

3.3 Drought forecasting

The selected ARIMA model (Eq. 17) was then used to forecast streamflow from January, 2000 to December, 2000. The forecasted and observed flow rates are compared first with two truncation levels, which are time series mean and monthly mean (Fig. 9). It is obvious that the period of January to December is a drought period. The ability of the selected model to forecast drought is also clear from the figure. Both observed and forecasted series are below the truncation levels.

The SSFI is calculated for both forecasted and observed time series using Eq. 14. Table 4 shows the classification of SSFI. The comparison between observed and forecasted SSFI is shown in Fig. 10. The

Table 3 Test results for the comparison between forecasted and observed series at 95% confidence level

Forecasting scenario	Correlation coefficient	Coefficient of efficiency	RMSE	Wilcoxon's <i>P</i> -value	Levene's <i>P</i> -value	K-S test
Scenario 1	0.577	0.165	15.82	0.007	0.009	0.004
Scenario 2	0.795	0.605	2.12	0.031	0.019	0.021
Scenario 3	0.925	0.971	0.42	0.202	0.148	0.536

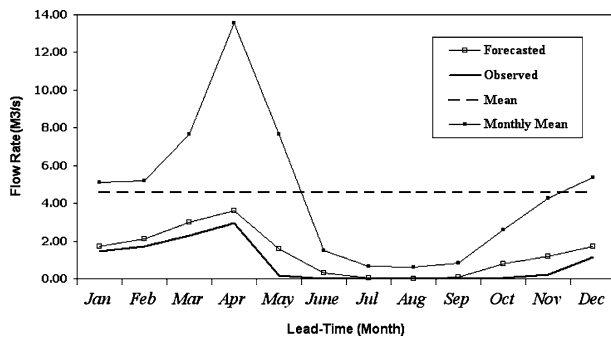


Fig. 9 Comparison of observed, forecasted and two drought truncation levels

Table 4 Drought Classification based on SPI-value

Classification	SPI
Extremely wet	SPI > 2
Very wet	1.5 < SPI < 1.99
Moderately wet	1.0 < SPI < 1.49
Near normal	-0.99 < SPI < 0.99
Moderately dry	-1.49 < SPI < -1.0
Severely dry	-1.99 < SPI < -1.5
Extremely dry	SPI < -2.0

SSFI can show the important feature of drought, “Severity.” Similar to SPI drought severity classification (McKee et al 1993; Mishra and Desei 2005), the severity of observed drought is also shown in Table 5. This table and Fig. 9 show a period of severe drought for January, February and December, moderate drought for March, April, October and November. The condition of May, June, July and August is near normal because these months are usually dry seasons in the

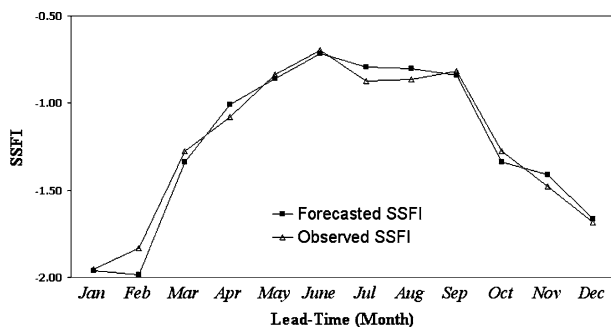


Fig. 10 Comparison of observed and forecasted standardized streamflow index

Table 5 Observed and forecasted SSFI and their classification

Lead-time	Forecasted SSFI	Observed SSFI	Classification
January	-1.96	-1.95	Severely dry
February	-1.99	-1.83	Severely dry
March	-1.34	-1.28	Moderately dry
April	-1.01	-1.08	Moderately dry
May	-0.86	-0.83	Near normal
June	-0.72	-0.70	Near normal
July	-0.79	-0.87	Near normal
August	-0.80	-0.87	Near normal
September	-0.84	-0.82	Near normal
October	-1.34	-1.28	Moderately dry
November	-1.41	-1.48	Moderately dry
December	-1.67	-1.68	Severely dry

study area. It is also clear that the ARIMA stochastic model is able to forecast drought in leading time, T_{n+1}, \dots, T_{n+1} , both in duration and severity. However, it should be noted that the accuracy in modeling is very important in obtaining a better result.

Hydrologic drought frequency analysis was applied as an alternative truncation level for drought forecasting. Different frequency distributions were fitted to monthly streamflow and the flow rate for hydrologic drought in different 2-, 5-, 10- and 20-year return periods were estimated using maximum likelihood method of quantile estimation. The results of quantiles (streamflow in different return periods) estimation are presented in Table 6 and the best frequency distribution was selected on the basis on minimum RMSE. Here, Eq. 12 is written as

$$RMSE = \left(\frac{\sum_{i=1}^n (F_i - O_i)}{n - p} \right)^{1/2} \tag{18}$$

where “*p*” is the number of distribution parameters. In this table, for example, if February streamflow is between 5 and 4.4 m³/s, a 2-year return period drought has occurred. If the observed streamflow is less than 3.7 m³/s, a drought event with return period more than 20-year return period has been occurred. Figures 11, 12, 13 and 14 show compare observed and forecasted values to the corresponding hydrologic drought for 2, 5, 10 and 20 year in different months.

For 2-year return period, both observed and forecasted streamflow are below the 2-year drought which

Table 6 Flow rate in different hydrologic drought return periods (T_r)

Month	Fitted distribution	$T_r = 2$ (m ³ /s)	$T_r = 5$ (m ³ /s)	$T_r = 10$ (m ³ /s)	$T_r = 20$ (m ³ /s)
January	Two-parameter gamma	5	3.8	2.5	2
February	Two-parameter gamma	5	4.4	4	3.7
March	Two-parameter gamma	7.2	6	4.5	3.4
April	Two-parameter gamma	12	10.6	5	4
May	Two-parameter gamma	5	3.8	0.5	0.2
June	Two-parameter gamma	1	0.7	0.2	0.1
July	Generalized Pareto	0.47	0.23	0.1	0.05
August	Two-parameter gamma	0.3	0.2	0.1	0.05
September	Two-parameter gamma	0.5	0.2	0.1	0.05
October	Two-parameter gamma	2.3	2	0.6	0.5
November	Two-parameter gamma	4	3.3	2	1.7
December	Two-parameter gamma	5.2	4.2	3	2.7

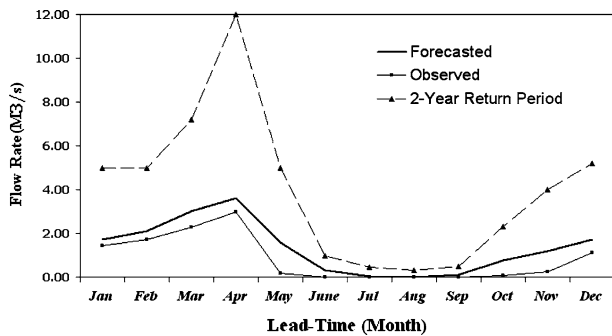


Fig. 11 Comparison between observed and forecasted streamflow with 2-year hydrologic drought

indicates that the region will experience a 2-year hydrologic drought for all months in 2000 year. The same condition can be seen for 5-year hydrologic drought (Fig. 12) which shows a more severely dry condition than that of 2-year drought.

In the case of 10- and 20-year hydrologic drought, Figs. 13 and 14 shows a slightly different condition. While both observed and forecasted streamflow shows a drought period from January to April comparing with 10- and 20-year hydrologic drought, forecasted drought for May does not match with observed drought condition. There may be additional water in

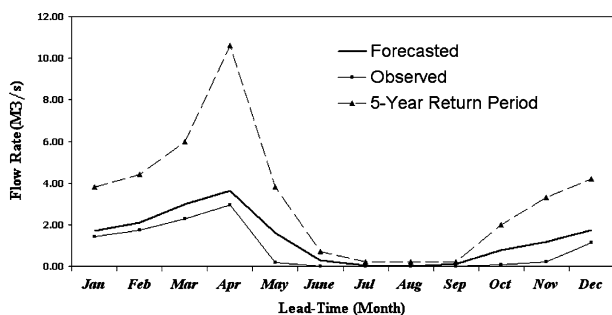


Fig. 12 Comparison between observed and forecasted streamflow with 5-year hydrologic drought

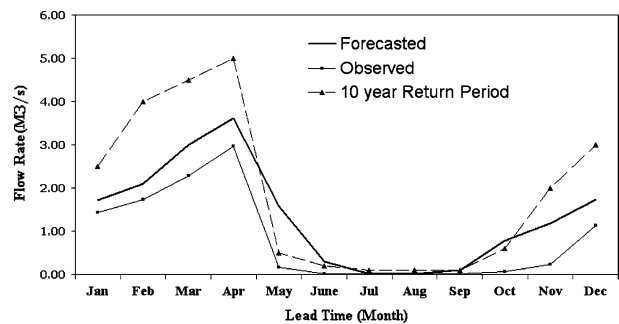


Fig. 13 Comparison between observed and forecasted streamflow with 10-year hydrologic drought

streamflow channel by snow melting. In general, it could be concluded that the forecasted monthly streamflow shows a period of water deficit and the managers of water resources should carefully decide on water resources planning and management in the leading time.

4 Conclusions

This study impels the capability of multiplicative AR-IMA model in streamflow forecasting. The largest

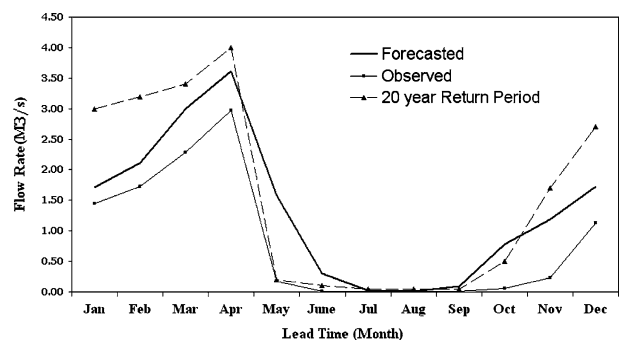


Fig. 14 Comparison between observed and forecasted streamflow with 20-year hydrologic drought

different (forecasting error) is observed in April and May and the smallest difference is observed in dry months between June and August. The higher difference in May and April is due to additional water flow by snowmelt. The capability of ARIMA model could also be seen from the analogy between monthly variation of forecasted and observed values where the highest streamflow happens in winter month and the lowest streamflow occurs in dry summer month. The comparison of observed and forecasted drought also proves the aptitude of ARIMA models for forecasting. However, it seems that the accuracy of drought forecasting depends on the selected threshold. Here, it depends on water resource managers and planners to choose a drought threshold according to the goal of drought study. This study showed that simple threshold like long-term mean is not suitable for drought analysis. A more intricate monthly mean is a better choice. However, a hydrologist or a planner would benefit from applying normalized streamflow drought index because the former index can also show the severity of drought that the planner is going to deal with. In other words, selecting some series or monthly mean can show water deficit while SSFI can give you an idea about drought severity, the very important characteristics of drought. On the other hand, when the manager or hydrologist contracts with the question of drought risk of a give project, it would be advisable to choose an alternative drought hydrologic frequency threshold to have an estimate of risk involved in the hydrologic project.

Finally, the careful fitting of a linear stochastic models to hydrologic time series such as streamflow and rainfall, with an accurate drought definition and threshold, will result in better drought preparedness plan in a region so as to ensure sustainable water resource planning within the basin.

Acknowledgements The author is grateful to two anonymous reviewers for their comments, which helped improve presentation significantly. The comments from Z. Sen, C. Chatfield and A. Mishra are also appreciated. The author also thanks George Christakos, the Editor-in-Chief of the journal of Stochastic Environmental Research and Risk Assessment.

References

- American Meteorological Society (AMS) (2004) Statement on meteorological drought. *Bull Am Meteorol Soc* 85:771–773
- Bonacci O (1993) Hydrological identification of drought. *Hydrol Process* 7:249–262
- Box GEP, Jenkins GM (1976) Time series analysis, forecasting and control, revised edn. Holden-Day, San Francisco
- Bowerman BL, O'Connell RT (1993) Forecasting and time series, an applied approach. Duxbury, Pasific Grove
- Brath A, Rosso R (1993) Adaptive calibration of a conceptual model for flash flood forecasting. *Water Resour Res* 29(8):2561–2572
- Breusch T, Pagan A (1979) A simple test of heteroscedasticity and random coefficient variation. *Econometrica* 47:1287–1294
- Chang TJ, Kleopa XA (1991) A proposed method for drought monitoring. *Water Resour Bull* 27:275–281
- Chang TJ, Stenson JR (1990) Is it realistic to define a 100-year drought for water management? *Water Resour Bull* 26:823–829
- Chung CH, Salas JD (2000) Drought occurrence probabilities and risks of dependent hydrological processes. *J Hydrol Eng ASCE* 5(3):259–268
- Clausen B, Pearson CP (1995) Regional frequency analysis of annual maximum streamflow drought. *J Hydrol* 173:111–130
- Conover WJ (1980) Practical nonparametric statistics, 2nd edn. Wiley, New York
- Delleur JW, Tao PC, Kavas ML (1976) An evaluation of practicality and complexity of some rainfall and runoff time series models. *Water Resour Res* 12(5):953–970
- Dracup JA, Lee KS, Paulson EG Jr (1980) On the definition of droughts. *Water Resour Res* 16:297–302
- Efron B, Tibshirani RJ (1993) An introduction to the bootstrap. Chapman and Hall, New York
- Griffiths GA (1990) Rainfall deficit: distribution of monthly runs. *J Hydrol* 115:219–229
- Hanson RT, Newhouse MW, Dettinger MD (2004) A methodology to assess relations between climatic variability and variations in hydrologic time series in the southwestern United States. *J Hydrol* 287:252–269
- Hipel KW (1993) Practical results in simulation and forecasting. In: Macro JB, Harboe R, Salas JD (eds) Stochastic hydrology and its use in water resources systems simulation and optimization. NATO Advanced Study Institute, Kluwer Academic Publishers, Dordrecht, Netherlands pp. 175–188
- Hipel KW, McLeod AE (1994) Time series modeling of water resources and environmental systems. Elsevier, Amsterdam, The Netherlands
- Hollander M, Wolfe DA (1999) Nonparametric statistical methods. Wiley, New York
- Khan MS, Coulibaly P, Dibike Y (2006) Uncertainty analysis of statistical downscaling methods. *J Hydrol* 319:357–382
- Kim T, Valdes JB (2003) Nonlinear model for drought forecasting based on a conjunction of wavelet transforms and neural networks. *J Hydrol Eng ASCE* 8(6):319–328
- Levene H (1960) Contributions to probability and statistics. Stanford University Press, Stanford
- Loaiciga HA, Leipnik RB (1996) Stochastic renewal model of low-flow stream sequences. *Stochastic Hydrol Hydraulics* 10(1):65–85
- Lohani VK, Loganathan GV (1997) An early warning system for drought management using the Palmer drought index. *J Am Water Resour Assoc* 33(6):1375–1386
- Loukas A, Vasilades L (2004) Probabilistic analysis of drought spatiotemporal characteristics in Thessaly region, Greece. *Nat Hazard Earth Syst Sci* 4:719–731
- McKee TB, Doesken NJ, Kleist J (1993) The relationship of drought frequency and duration to time scales. In: Proceedings of the 8th conference on applied climatology, Anaheim, American Meteorological Society, pp. 179–184
- Mishra AK, Desai VR (2005) Drought forecasting using stochastic models. *Stochastic Environ Res Risk Assess* 19:326–329

- Salas JD, Obeysekera JTB (1982) ARMA model identification of hydrologic time series. *Water Resour Res* 18(4):1011–1021
- Salas JD, Delleur JW, Yevjevich VM, Lane WL (1980) Applied modeling of hydrologic time series. Water Resources Publications, Littleton
- Sen Z (1976) Wet and dry periods of annual flow series. *J Hydraulics Div ASCE* 106(HY1):99–115
- Sen Z (1977) Run sums of annual flow series. *J Hydrol* 35:311–324
- Yevjevich V (1967) An objective approach to definitions and investigations of continental hydrologic droughts. *Hydrology Papers Colorado State University, Fort Collins*
- Yurekli K, Kurunc K, Ozturk F (2005) Application of linear stochastic models to monthly flow data of Kelkit Stream. *Ecol Model* 183:67–75
- Wilhite DA, Glantz MH (1985) Understanding the drought phenomenon: the role of definitions. *Water Int* 10:111–120
- Wilhite DA, Rosenberg NJ, Glantz MH (1986) Improving federal response to drought. *J Clim Appl Meteorol* 25:332–342
- Zelenhasic E, Salvai A (1987) A method of streamflow drought analysis. *Water Resour Res* 23:156–168